

# Dark Matter Capture in the First Stars: a Power Source and limit on Stellar Mass

Katherine Freese<sup>1,3</sup>, Douglas Spolyar<sup>2</sup>, and Anthony Aguirre<sup>2</sup>

February 26, 2019

## Abstract

Weakly interacting massive particles, which are their own antiparticles, can annihilate and provide an important heat source for the first (zero-metallicity) stars. The luminosity from dark matter (DM) annihilation may dominate over the luminosity due to fusion, depending on the DM density. Even more interesting is the possibility that the DM annihilation may exceed the Eddington luminosity and prevent the first stars from growing beyond a limited mass. Alternatively, if heavy zero-metallicity stars are found, they may be used to bound dark matter properties.

## 1 Introduction

The first stars in the Universe mark the end of the cosmic dark ages, reionize the Universe, and provide the enriched gas required for later stellar generations. They may also be important as precursors to black holes that coalesce and power bright early quasars. The first stars are thought to form inside halos of dark matter of mass  $10^5 M_\odot$ – $10^6 M_\odot$  at redshifts  $z = 10$ – $50$ . These halos consist of 85% dark matter and 15% baryons in the form of pristine hydrogen and helium (from Big Bang nucleosynthesis). The baryonic matter cools and collapses via molecular hydrogen cooling [1, 2, 3] into a single small protostar [4] at the center of the halo (for reviews see e.g. [5, 6, 7]).

In this Letter we consider the effect of dark matter (DM) particles on the first stars. We focus on the most compelling dark matter candidate, the Weakly Interacting Massive Particles (WIMPs). WIMPs are the favorite dark matter candidate of many physicists because they automatically provide the right amount of dark matter, i.e. 24% of the energy density of the Universe. WIMPs are their own antiparticles, and annihilate with themselves in the early universe to produce the relic density today. The best example of a WIMP is the lightest supersymmetric particle. In particular, the neutralino, the supersymmetric partner of the  $W$ ,  $Z$ , and Higgs bosons, has the required weak interaction

cross section and  $\sim$  GeV - TeV mass to give the correct amount of dark matter. For a review of SUSY dark matter see [19].

It is this same annihilation process that is the basis of the work we consider here. WIMPs annihilate with one another wherever their density is high enough. Such high densities are achieved in the early Universe, in galactic halos today [8, 9], in the Sun [10] and Earth [11, 12], and, as we will show, also in the first stars. As our canonical values, we will use the standard value  $\langle\sigma v\rangle = 3 \times 10^{-26} \text{cm}^3/\text{sec}$  for the annihilation cross section and  $m_\chi = 100$  GeV for the WIMP particle mass, but will also consider a broader range of WIMP masses (1 GeV–10 TeV) and cross-sections<sup>1</sup>. The effects we find apply equally well to other WIMP candidates, such as sterile neutrinos or Kaluza-Klein particles.

In this paper we consider the effects of WIMP annihilation on the first stars. In a previous paper [14] two of us (together with P. Gondolo) considered the effects of dark matter annihilation on the formation of the first stars. We found that a crucial transition takes place when the gas density of the collapsing protostar exceeds a critical value ( $10^{13} \text{cm}^{-3}$  for a 100 GeV WIMP mass): at this point WIMP annihilation in the first protostellar clouds dominates over all cooling mechanisms and prevents the further collapse of the star. We suggested that the very first stellar objects are “dark stars,” a new phase of stellar evolution. In the dark stars, the DM only supplies 1% of the mass density and yet its annihilation provides the power source for the star. We are as yet uncertain of the lifetime of these dark stars. It is possible that they last as long as 600 Myr, which is the timescale for all the DM to annihilate away inside of the dark star without refilling the DM density from with DM from the halo outside of the dark star. In principle, the dark star may only be a transient phase. We suspect that eventually, the first stars are able to continue their collapse and return to the standard fusion driven Pop III stars. It is these Pop III stars that we consider in this paper.

Previous work on DM annihilation powering stars has also been done in the context of high DM densities near the supermassive black holes in galactic centers, e.g. WIMP burners [15] and more generally [16].

In this paper, we consider the effects of DM annihilation on early zero-metallicity (Population III) stars, once they do have fusion inside their cores. These stars live inside a reservoir of WIMPs; as the WIMPs move through the stars, some of the WIMPs are captured by the stars. The captured DM continues to scatter toward the center of the stars, where the DM can annihilate very efficiently, which has the effect of dramatically increasing the annihilation rate inside of a star compared to DM annihilation without scattering as was

---

<sup>1</sup> The interaction strengths and masses of the neutralino depend on a large number of model parameters. In the minimal supergravity model, experimental and observational bounds restrict  $m_\chi$  to 50 GeV–2 TeV, while  $\langle\sigma v\rangle$  lies within an order of magnitude of  $3 \times 10^{-26} \text{cm}^3/\text{sec}$  (except at the low end of the mass range where it could be several orders of magnitude smaller). Nonthermal particles can have annihilation cross-sections that are many orders of magnitude larger (e.g. [13]) and would have even more drastic effects.

considered in [14]<sup>2</sup>. Regardless, the annihilation provides a heat source for the stars. We compare the DM annihilation luminosity due to capture to the fusion luminosity of the stars, as well as to the Eddington luminosity. Thus, even though DM annihilation may fail to stop a POPIII star from forming, DM can nonetheless effect the stars fate.

Just as we were preparing to submit our paper, a very similar work was submitted by [17]. However, we have carried the analysis further. We agree with [17] in the conclusion that DM annihilation may dominate over fusion and we illustrate the DM densities required for this conclusion. In addition, we go one step further and discuss the possibility that the DM power source may exceed the Eddington luminosity and prevent the first stars from growing beyond a limited mass, which would effect the IR background, the re-ionization of the universe, the number of supernova and potentially the type of supernova of the first stars which will be addressed in a separate publication[21]

We begin by discussing the WIMP abundance in the first stars. To do this we need to compute the number of WIMPS captured by the first stars, and compare with the annihilation rate of WIMPs in the first stars. A discussion of adiabatic contraction, which may drive up the DM density near the baryons, follows. Then we compute the DM annihilation luminosity and compare with fusion luminosity. Finally, we compare the DM luminosity with the Eddington luminosity and find a maximum stellar mass as a function of DM density.

## 2 WIMP Abundance

As WIMPs travel through a star, they can scatter off of the nuclei in the star with the scattering cross section  $\sigma_c$ . Although most of the WIMPs travel right through the star, some of them lose enough energy to be captured. We call the capture rate  $C(sec^{-1})$ . The WIMPs then sink to the center of the star, where they can annihilate with one another with the annihilation rate  $\Gamma_A(sec^{-1})$ . This process was previously noticed as important for the Sun by [10] and in the Earth by [11, 12]; there the annihilation products may provide a way to discover WIMPs via indirect detection (e.g.  $\gamma$ -rays in GLAST,  $e^+$  in PAMELA, neutrinos in ICECUBE).

The number of WIMPs  $N$  in the star is then determined by a competition between capture and annihilation via the differential equation,  $\dot{N} = C - C_A N^2$  where the second term on the right hand side is twice the annihilation rate of DM captured in the star,  $\Gamma_A = \frac{1}{2}C_A N^2$ . The solution to this equation is  $\Gamma_A = \frac{1}{2}C \tanh^2(t/\tau)$ . Here

$$\tau = (CC_A)^{-1/2} \tag{1}$$

---

<sup>2</sup>We note that DM does annihilate in the WIMP reservoir. Since the star sits inside of the reservoir, some DM will annihilate inside of the star without capture

$M_*(M_\odot)$	$T(K)$	$\rho(g/cm^3)$	$V_2/V_1^2(cm^{-3})$	$C_A(sec^{-1})$
Sun	-	-	$1.72 \times 10^{-28}$	$5.16 \times 10^{-54}$
10	$9.55 \times 10^7$	225.8	$1.77 \times 10^{-29}$	$5.31 \times 10^{-55}$
50	$1.13 \times 10^8$	48.63	$1.38 \times 10^{-30}$	$4.14 \times 10^{-56}$
100	$1.18 \times 10^8$	31.88	$6.86 \times 10^{-31}$	$2.06 \times 10^{-56}$
250	$1.23 \times 10^8$	19.72	$3.11 \times 10^{-31}$	$9.33 \times 10^{-57}$

Table 1: We have given the central temperature  $T(K)$  and central baryon density  $\rho(g/cm^3)$  for various masses of metal free stars half way through hydrogen burning [20]. We also calculated the effective volume  $V_2/V_1^2$ . Please note that the annihilation rate of captured DM is simply  $\Gamma_a = 1/2C_A N^2$  where  $N$  is the number of DM particle captured in the star. Please note that entry marked Sun refers to the present day Sun. We have also used the fiducial values to calculate the last two columns. Namely,  $m_\chi = 100(GeV)$ , and  $\langle \sigma_{ann} v \rangle = 3 \times 10^{-26}(cm^3/sec)$ .

is the equilibrium time which is reached once the capture rate balances the annihilation rate of captured DM,

$$\Gamma_A = \frac{1}{2}C; \quad (2)$$

the factor of 2 is due to the fact that two WIMPs are needed to annihilate whereas only one is needed for scattering. As we will show, for the case of Pop III stars, equilibrium is quickly reached ( $t \gg \tau$ ) and we may use Eq.(2).

*Annihilation Rate:* The quantity  $C_A$  depends on the WIMP annihilation cross section and the distribution of WIMPs in the star, which have been captured[18],

$$C_A = \langle \sigma v \rangle_{ann} \frac{V_2}{V_1^2} \quad (3)$$

where

$$V_j = [3m_{pl}^2 T / (2jm_\chi \rho)]^{3/2}, \quad (4)$$

where  $T$  is the core temperature of the star,  $m_{pl}$  is the Planck mass, and  $\rho$  is the core density of the star.

In Table 1, we have computed  $C_A$  in Pop III stars of different masses. From S. Woosley [20], we have obtained the properties of zero metallicity stars when they are halfway through hydrogen burning on the main sequence. For the annihilation cross section we use the standard

$$\langle \sigma v \rangle_{ann} = 3 \times 10^{-26} cm^3/sec \quad (5)$$

as this gives the right WIMP relic density today. The numbers in the plot are obtained using the canonical 100 GeV WIMP mass, but can easily be scaled to any other WIMP mass since  $C_A \propto m_\chi^{1.5}$ .

*Capture Rate:* WIMP interactions with nuclei are of two kinds: spin-independent, which scales as  $A^2$  (where  $A$  is the number of nucleons in the nucleus), and spin-dependent, which require the nucleon to have a spin. Currently the direct detection experimental bounds on elastic scattering are the weakest for the spin-dependent contribution (to be precise we are considering only scattering off of protons), roughly (see figure 2) [22]  $\sigma_{c,SD} \leq 10^{-37}\text{cm}^2$  for  $m_\chi = 100\text{GeV}$  or  $\sigma_{c,SD} \leq 10^{-36}\text{cm}^2$  for  $m_\chi = 1\text{TeV}$ . The bound on the spin-independent scattering is much tighter,  $\sigma_{c,SI} \leq 10^{-42}\text{cm}^2$  for  $m_\chi = 100\text{GeV}$  (CDMS,XENON). We have ignored bounds from indirect detection experiments for they are model dependent, but they at most limit  $\sigma_c < 10^{-38}(\text{cm}^2)$ , which does not dramatically alter our results. The first stars are made only of hydrogen or helium so that the  $A^2$  enhancement for the spin-independent contribution is not substantial. In this paper we consider only the spin-dependent contribution, though in principle for any specific candidate WIMP one should self-consistently include both. As our fiducial value, in this paper we use the spin-dependent cross section

$$\sigma_c = 10^{-37}\text{cm}^2 \quad (6)$$

but will always show the dependence of any result on the value of  $\sigma_c$ .

The capture rate per unit volume at a distance  $r$  from the center of the star, for an observer at rest with respect to the WIMPs which we assume to be true to first order, is [23]

$$\frac{dC}{dV}(r) = \left(\frac{6}{\pi}\right)^{1/2} nn_\chi(\sigma_c\bar{v})\frac{v(r)^2}{\bar{v}^2} \left[1 - \frac{1 - \exp(-B^2)}{B^2}\right] \quad (7)$$

where  $n$  is the number density of nucleons (here, hydrogen),  $n_\chi$  is the WIMP number density,  $v(r)$  is the escape velocity of WIMPs from the star at a given radius  $r$ , and  $\bar{v}^2 \equiv \frac{3kT_\chi}{M}$  is a “velocity dispersion” of WIMPs in the DM halo. Also please note that the probability of scattering goes like  $nn_\chi(\sigma_c\bar{v})$  while the other factors in eq.7 reflect the probability of being captured after scattering. Also,

$$B^2 \equiv \frac{3}{2} \frac{v(r)^2}{\bar{v}^2} \frac{\mu}{\mu_-} \quad (8)$$

where

$$\mu = \frac{m_\chi}{M_N} \quad (9)$$

is the ratio of WIMP to nucleon mass and

$$\mu_- = (\mu + 1)/2. \quad (10)$$

For an observer moving with respect to the WIMPs, the quantity in square brackets in Eq.(7) becomes a more complicated function of  $B$  and the relative velocity as shown in Eq.(2.24) in [23].

The capture rate for the entire star is then

$$C = \int_0^{R_*} 4\pi r^2 \frac{dC}{dV}(r), \quad (11)$$

where  $R_*$  is the radius of the star. To obtain a conservative estimate of the capture rate, we may take

$$v(r) = v(R_*) \equiv v_{esc} = \frac{2GM_*}{R_*} \quad (12)$$

for all  $r$ . In this case the integral simplifies and we find

$$C = \left(\frac{6}{\pi}\right)^{1/2} \left(\frac{M_*}{m_p} f_H\right) (\sigma_c \bar{v}) \left(\frac{v_{esc}}{\bar{v}}\right)^2 \frac{\rho_\chi}{m_\chi}, \quad (13)$$

where  $M_*$  is the stellar mass,  $m_p$  is the proton mass and  $f_H$  is the fraction of the star in hydrogen. n.b. hydrogen has spin while Helium generally does not have spin. We could in principle consider the spin-independent contribution of scattering off of hydrogen and helium in the stars as well, but have not done so as we believe them to be subdominant; in any case the current work is conservative in considering only the spin-dependent contribution.

To estimate  $\bar{v}$  [24], we take the virial velocity of the DM halo,

$$\langle \bar{v}^2 \rangle = \frac{|W|}{M_{halo}} \quad (14)$$

where

$$W = -4\pi G \int \rho_{halo} M_{halo} r dr \quad (15)$$

and the typical DM halo containing a Pop III star has  $M_{halo} = 10^6 - 10^7 M_\odot$  where  $M_\odot$  is the mass of the Sun. We use a Navarro Frenk White (NFW) profile [27] for the DM,

$$\rho_{halo} = \frac{\rho_0}{\frac{r}{r_s} \left(1 + \frac{r}{r_s}\right)^2} \quad (16)$$

where  $r_s$  is the scale radius. The normalization  $\rho_0$ , known as the central density, depends on the concentration parameter  $C_{vir}$  which ranges from  $C_{vir} = (1 - 10)$  and on the redshift which ranges from  $z = 10 - 30$ . With  $r_s$  in the range (15-100) pc. we find  $\bar{v} = (1 - 15)$ km/sec. As our fiducial value, we will take

$$\bar{v} = 10\text{km/sec.} \quad (17)$$

For a star at rest, one can show that the term in square brackets in Eq.(7) is very close to 1. This is true for  $B \gg 1$ . For example, for a  $1M_\odot$  star, we have  $v_{esc} = 618\text{km/sec}$ ,

$M_*(M_\odot)$	$R_*(R_\odot)$	$V_{esc}(V_\odot)$	$C(sec^{-1})$	$\tau(yrs)$
Sun	1	1	$4.9 \times 10^{35}$	20
10	1.16	2.49	$8.1 \times 10^{35}$	48
50	4.76	3.24	$6.8 \times 10^{36}$	60
100	7.04	3.77	$1.9 \times 10^{37}$	50
250	11.8	4.60	$6.9 \times 10^{37}$	40

Table 2: We have characterized the star’s mass ( $M_*$ ), radius ( $R_*$ ), and surface escape velocity ( $V_{esc}$ ) in solar units, which are determined for metal free stars halfway through hydrogen burning. We have also calculated the capture rate  $C$  using our fiducial values  $\rho_\chi = 10^8(GeV/cm^3)$ ,  $m_\chi = 100(GeV)$ , and  $\sigma_c = 10^{-37}(cm^2)$  and  $\tau$  by using  $C_A$  from Table 1. As in Table 1, the entry marked Sun refers to the present day sun and not a zero metallicity star. The capture rate for the sun still uses the fiducial values. Also the capture rate in the present day sun is much smaller  $C \approx 10^{24}(sec^{-1})$  mostly due to the much lower DM densities in the solar neighborhood.

which is much larger than  $\bar{v} = 10\text{km/sec}$ . Using these values and e.g. for  $m_\chi = 100$  GeV,  $B \sim 100$ . The fact that  $B \gg 1$  holds for all stellar and WIMP masses we are considering so that we may ignore the term in square brackets. Similarly, for a star moving through the WIMP halo, the factor that replaces the term in square brackets is  $O(1)$ . For example, for a  $1 M_\odot$  star and  $m_\chi = 100$  GeV, the factor is 0.66. We note that, in today’s stars, this factor is much more important than in the first stars because  $\bar{v}$  is much larger today (due to the fact that today’s galactic haloes are much larger, e.g.  $10^{12}M_\odot$ ).

In Table II, we evaluate the capture rate in Eq.(13), again using properties (including stellar radius) of Pop III stars from [20]. In obtaining these numbers, we have used  $\rho_\chi = 10^8$  GeV/cm<sup>3</sup>,  $m_\chi=100$  GeV, and  $\sigma_c = 10^{-37}\text{cm}^2$ ; the result can easily be scaled to other values since  $C \propto \rho_\chi \sigma_c / m_\chi$ . As a rough approximation, we may write the capture rate as

$$C \sim 4.9 \times 10^{35} \text{sec}^{-1} \left( \frac{M_*}{M_\odot} \right) \left( \frac{v_{esc}}{618 \text{km/sec}} \right)^2 \left( \frac{\bar{v}}{10 \text{km/sec}} \right)^{-1} \left( \frac{\rho_\chi}{10^8 \text{GeV/cm}} \right) \left( \frac{m_\chi}{100 \text{GeV}} \right)^{-1} \left( \frac{\sigma_c}{10^{-37} \text{cm}^2} \right). \quad (18)$$

Using Eq.(12) and noting that for the Pop III models of [20] it is roughly true that  $R_* \propto M_*^{0.45}$ , we find that approximately

$$C \sim 4.9 \times 10^{35} \text{sec}^{-1} \left( \frac{M_*}{M_\odot} \right)^{1.55} \left( \frac{\bar{v}}{10 \text{km/sec}} \right)^{-1} \left( \frac{\rho_\chi}{10^8 \text{GeV/cm}} \right) \left( \frac{m_\chi}{100 \text{GeV}} \right)^{-1} \left( \frac{\sigma_c}{10^{-37} \text{cm}^2} \right). \quad (19)$$

Table II also shows the equilibrium timescale given by Eq.(1) using the capture and annihilation rates determined above. We can see that  $\tau$  is very short, i.e. tens of years. Hence for most of the lifetime of the zero metallicity stars,  $t \gg \tau$  and we may use Eq.(2).

*DM density profile.* — To study the effects of dark matter on the first stars, we need to know density of the DM passing through the stars to determine the capture rate. Simulations have unfortunately (as yet) not resolved this issue. Below we will use a variety of DM densities, since these numbers are unknown. In our previous paper [14], we used adiabatic contraction [26] to obtain estimates of the DM profile. Prior to this contraction, we assume an overdense region of  $10^5 M_\odot$ – $10^6 M_\odot$  with a Navarro-Frenk-White (NFW) profile [27] for both DM and gas, where the gas contribution is 15%. (For comparison, we also used a Burkert profile [28], which has a DM core before contraction.) As the gas collapses, we allowed the DM to respond to the changing baryonic gravitational potential, where the gas density profiles were taken from simulations of [29, 30]). The final DM density profiles were computed with adiabatic contraction [ $M(r)r = \text{constant}$ ]. After contraction, we found a DM density at the outer edge of the baryonic core of roughly  $\rho_\chi \simeq 5 \text{GeV}/\text{cm}^{-3} (n/\text{cm}^3)^{0.81}$  which scales as  $\rho_\chi \propto r^{-1.9}$  outside the core (see Fig. 1 in [14]). Our adiabatically contracted NFW profiles match the DM profile obtained numerically in [29] (see their Fig. 2). They present their earliest (gas core density  $n \sim 10^3 \text{cm}^{-3}$ ) and latest ( $n \sim 10^{13} \text{cm}^{-3}$ ) DM profiles, as far inward as  $5 \times 10^{-3} \text{pc}$  and  $0.1 \text{pc}$ . The slope of these two curves is the same as ours. If one extrapolates them inward to smaller radii, one obtains the same DM densities as with our adiabatic contraction approach. The highest DM density found by [29] was  $10^8 \text{GeV}/\text{cm}^3$ . Should the adiabatic contraction continue all the way to the small stellar cores at  $n \sim 10^{22} \text{cm}^{-3}$  (which we doubt), the DM density would be as high as  $10^{18} \text{GeV}/\text{cm}^3$ . We note that [31] obtained DM density profiles in galaxies and found that adiabatic contraction produces densities that are too high by only a factor of 2 or 3, even when radial orbits are included, or in the presence of bars, or in the absence of spherical symmetry. Below we will use a variety of DM densities due to the uncertainties.

### 3 Luminosity due to WIMP annihilation:

We may now compute the luminosity due to WIMP annihilation,

$$L_{DM} = f \Gamma_A m_\chi, \quad (20)$$

where we taken the energy per annihilation to be the WIMP mass and  $f$  is the fraction of annihilation energy that goes into the luminosity. Roughly 1/3 of the annihilation energy is lost to neutrinos that stream right out of the star, whereas the other 2/3 goes into electrons, positrons, and photons that get stuck in the star. Hence we take

$$f \sim 2/3. \quad (21)$$

For  $t \gg \tau$ , which is quickly reached, Eq.(20) may be rewritten using Eq.(2) as

$$L_{DM} = \frac{f}{2} C m_\chi. \quad (22)$$



$M_*(M_\odot)$	$L_*(Ergs/sec)$	$L_{DM}(Ergs/sec)$	$\rho_\chi(GeV/cm^3)$ for which $L_* = L_{DM}$
Sun	$3.9 \times 10^{33}$	$1.3 \times 10^{34}$	$3 \times 10^7$
10	$4.2 \times 10^{37}$	$8.1 \times 10^{35}$	$5.3 \times 10^9$
50	$2.0 \times 10^{39}$	$6.8 \times 10^{36}$	$3.0 \times 10^{10}$
100	$6.45 \times 10^{39}$	$1.9 \times 10^{37}$	$3.3 \times 10^{10}$
250	$2.31 \times 10^{40}$	$6.9 \times 10^{37}$	$3.4 \times 10^{10}$

Table 3: We are still considering the stars as previously defined in the previous tables. We have again taken the fiducial values, except in the final column where we vary  $\rho_\chi$  to determine when the DM luminosity  $L_{DM}$  exceeds the luminosity of the star in the absence of DM annihilation  $L_*$ . The third column gives  $L_{DM}$  with our fiducial values.

The WIMP luminosity is given in Table III for a variety of stellar masses together with the ordinary fusion-powered stellar luminosity  $L_*$  provided by the models of [20] for these stars. Roughly, using Eq.(19) we may write

$$L_{DM} = 1.3 \times 10^{34} \text{erg/sec} \left( \frac{M_*}{M_\odot} \right)^{1.55} \left( \frac{\rho_\chi}{10^8 \text{GeV/cm}^3} \right) \left( \frac{\sigma_c}{10^{-37} \text{cm}^2} \right). \quad (23)$$

The WIMP luminosity depends linearly on the the WIMP density passing through the stars. We have also computed the WIMP energy density  $\rho_{\chi,crit}$  that is required in order for the WIMP annihilation energy to equal the ordinary stellar luminosity, which will dramatically alter the properties of the first stars[21]. For any WIMP densities higher than this value, the star's luminosity is dominated by annihilation energy (rather than by ordinary fusion). We note that the luminosity due to fusion scales as  $L_{fusion} \propto M^3$  whereas  $L_{DM} \propto M^{1.55}$ . Yet the fusion luminosity is subdominant for the values of  $\rho_{\chi,crit}$  given in the last column of Table III, and is subdominant for all stellar masses for  $\rho_\chi > 4 \times 10^{10} \text{GeV/cm}^3$ . See Figure 1.

## 4 Eddington luminosity

The Eddington luminosity is defined [25] to be

$$L_{Edd} = \frac{4\pi c G M_*}{\kappa_p} \quad (24)$$

where  $G$  is Newton's Constant,  $c$  is the speed of light,  $M_*$  is the mass of the star, and  $\kappa_p$  is the opacity of stellar atmosphere. Since the stellar atmosphere of the first stars are hot, the opacity is dominated by Thompson scattering, so we take

$$L_{Edd} = 1.4 \times 10^{38} (M_*/M_\odot) = 3.5 \times 10^4 (M_*/M_\odot) L_\odot. \quad (25)$$

In Figure 1, we have plotted three luminosities as a function of stellar mass for zero metallicity stars: the luminosity due to fusion, the luminosity due to WIMP annihilation (for a variety of WIMP densities in the star), and the Eddington luminosity. Since the Eddington luminosity scales as  $L \propto M_*$  whereas the DM luminosity scales as  $L_{DM} \propto M_*^{1.55}$ , for a large enough dark matter density the two curves will cross for some stellar mass. Once we find the lightest stellar mass for which  $L_{DM} > L_{Edd}$ , then the star of that mass is unable to accrete any further. The radiation pressure from the WIMP annihilation blows off any additional mass. Then there is an upper limit to the mass of the first stars. For example, we find that for a dark matter density of  $\rho_\chi = 10^{12} \text{ GeV/cm}^3$ , the DM luminosity exceeds  $L_{Edd}$  for any stellar mass heavier than  $1M_\odot$ . In other words, for this WIMP density the first stars cannot be more massive than  $1M_\odot$ .

Figure 2 illustrates the maximum stellar mass  $M_*^{\text{max}}$  as a function of WIMP energy density in the star for several values of the scattering cross section. Figure 3 is a plot of WIMP scattering cross section vs. WIMP mass. Experimental bounds are shown. In addition, the horizontal lines indicate the values of  $\sigma_c$  that correspond to different values of  $\rho_\chi$  at which a  $1 M_\odot$  star is Eddington limited by DM annihilation. The scaling to other stellar masses is straightforward since  $L_{DM} \propto M_*^{1.55}$ .

These arguments can be turned around to place a bound on the scattering cross section. If first stars of various masses are found, then one could rule out any combination of  $\sigma_c$  and  $\rho_\chi$  for a given WIMP mass that would not allow stars of such a mass to form. As an extreme example, if one were to believe adiabatic contraction all the way to the limit where the protostellar core has gas density  $n \sim 10^{22} \text{ cm}^{-3}$ , the WIMP density would reach  $\rho_\chi = 10^{18} \text{ GeV/cm}^3$ . In this case the Eddington limit would be reached for masses  $\ll 1M_\odot$  for our fiducial scattering cross section. If, instead, the first stars are observed to form with stars with masses larger one solar mass, and such an enormous WIMP density were found to be sensible, one could place a bound of  $\sigma_c < 10^{-43} \text{ cm}^2$  on WIMPs for almost any mass since the DM luminosity is independent of mass, the tightest known bound on the scattering cross section.

We thank S. Woosley for sharing with us his models of zero metallicity stars. We also thank J. Primack and S. Profumo for useful discussions. We acknowledge support from: the DOE and MCTP via the Univ. of Michigan, the Perimeter Institute (K.F.), NSF grant AST-0507117 and GAANN (D.S.). K.F. acknowledges the hospitality of the Physics Dept. at the Univ. of Utah.

## References

- [1] P. J. E. Peebles and R. H. Dicke, *Astrophys. J.* **154**, 891 (1968).

- [2] T. Matsuda, H. Sato and H. Takeda, Prog. Theor. Phys. **46**, 416 (1971).
- [3] D. Hollenbach and C. F. McKee, Astrophys. J. Suppl. Ser. **41**, 555 (1979).
- [4] K. Omukai and R. Nishi, Astrophys. J. **508**, 141 (1998).
- [5] E. Ripamonti and T. Abel, arXiv:astro-ph/0507130.
- [6] R. Barkana and A. Loeb, Phys. Rep. **349**, 125 (2001).
- [7] V. Bromm and R. B. Larson, Annu. Rev. Astron. Astrophys. **42**, 79 (2004).
- [8] J. R. Ellis *et al.*, Phys. Lett. B **214**, 403 (1988).
- [9] P. Gondolo and J. Silk, Phys. Rev. Lett. **83**, 1719 (1999).
- [10] M. Srednicki, K. A. Olive, and J. Silk, Nucl. Phys. **B279**, 804 (1987).
- [11] K. Freese, Phys. Lett. **167B**, 295 (1986).
- [12] L. M. Krauss, M. Srednicki, and F. Wilczek, Phys. Rev. D **33**, 2079 (1986).
- [13] T. Moroi and L. Randall, Nucl. Phys. **B570**, 455 (2000).
- [14] K. Freese, P. Gondolo and D. Spolyar, arXiv:0709.2369 [astro-ph].
- [15] I. V. Moskalenko and L. L. Wai, Astrophys. J. **659**, L29 (2007) [arXiv:astro-ph/0702654].
- [16] P. Scott, J. Edsjo and M. Fairbairn, arXiv:0711.0991 [astro-ph].
- [17] F. Iocco, arXiv:0802.0941 [astro-ph].
- [18] K. Griest and D. Seckel, Nucl. Phys. B **283**, 681 (1987) [Erratum-ibid. B **296**, 1034 (1988)].
- [19] G. Jungman, M. Kamionkowski and K. Griest, Phys. Rept. **267**, 195 (1996) [arXiv:hep-ph/9506380].
- [20] Private communication.
- [21] Work in progress.
- [22] C. Savage, P. Gondolo and K. Freese, Phys. Rev. D **70**, 123513 (2004) [arXiv:astro-ph/0408346].
- [23] A. Gould, Astrophys. J. **328**, 919 (1988).
- [24] J. Binney, S. Tremaine, 1987, Galactic Dynamics, Princeton University Press.
- [25] C. J. Hansen, S. D. Kawaler, V. Trimble, 2004 Stellar Interiors, 2nd Ed., Springer-Verlag.

- [26] G. R. Blumenthal *et al.*, *Astrophys. J.* **301**, 27 (1986).
- [27] J. F. Navarro, C. S. Frenk and S. D. M. White, *Astrophys. J.* **462**, 563 (1996).
- [28] A. Burkert, IAU Symposium/Symp-Int. Astron. Union **171**, 175 (1996); *Astrophys. J.* **447**, L25 (1995).
- [29] T. Abel, G. L. Bryan and M. L. Norman, *Science* **295**, 93 (2002).
- [30] L. Gao *et al.*, *Mon. Not. R. Astron. Soc.* **378**, 449 (2007).
- [31] J. A. Sellwood and S. S. McGaugh, *Astrophys. J.* **634**, 70 (2005) [arXiv:astro-ph/0507589].
- [32] G. Steigman *et al.*, *Astron. J.* **83**, 1050 (1978).
- [33] D. Merritt, arXiv:astro-ph/0301257.
- [34] E. Ripamonti, M. Mapelli and A. Ferrara, *Mon. Not. Roy. Astron. Soc.* **375**, 1399 (2007).
- [35] X. L. Chen and M. Kamionkowski, *Phys. Rev. D* **70**, 043502 (2004).
- [36] P. Gondolo *et al.*, *J. Cosmol. Astropart. Phys.* **7**, 8 (2004).
- [37] N. Fornengo, L. Pieri, and S. Scopel, *Phys. Rev. D* **70**, 103529 (2004).
- [38] W. M. Yao *et al.* (Particle Data Group), *J. Phys. G* **33**, 1 (2006).
- [39] B. Rossi, *High-Energy Particles* (Prentice-Hall, Inc., Englewood Cliffs, NJ, 1952).
- [40] M. Tegmark *et al.*, *Astrophys. J.* **474**, 1 (1997).
- [41] N. Yoshida *et al.*, *Astrophys. J.* **652**, 6 (2006).
- [42] S. W. Stahler, F. Palla, and E. E. Salpeter, *Astrophys. J.* **308**, 697 (1986).
- [43] J. C. Tan and C. F. McKee, *Astrophys. J.* **603**, 383 (2004).
- [44] Y. X. Li *et al.*, arXiv:astro-ph/0608190.
- [45] F. I. Pelupessy, T. Di Matteo and B. Ciardi, arXiv:astro-ph/0703773.

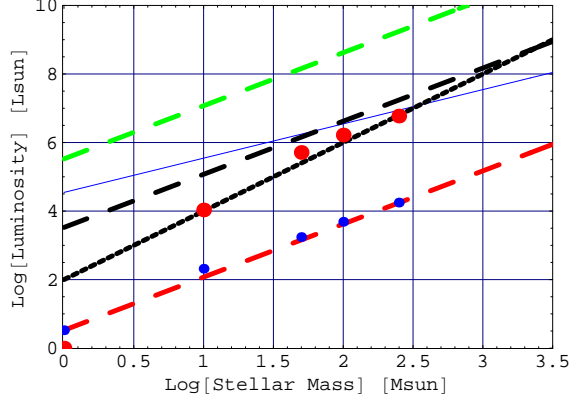


Figure 1: Log-Log plot of stellar mass versus luminosity in stellar units. Eddington luminosity (thin blue line), stellar luminosity as function of mass for zero metallicity stars (thick black line), large red dots Data points for zero metallicity stars in Table 3. We remind the reader that the lowest lying red dot is the Sun and not a zero metallicity star. Small red dots are from the second column of Table 3. Lowest lying Red dashed line is our fiducial example with  $\rho_\chi = 10^8 (GeV/cm^3)$  and  $\sigma_c = 10^{-37} (cm^2)$ , If we keep the cross section fixed, the middle dashed line corresponds to a DM density of  $10^{11} (GeV/cm^3)$ , and the top green dashed line would have a DM density of  $10^{13} (GeV/cm^3)$ .

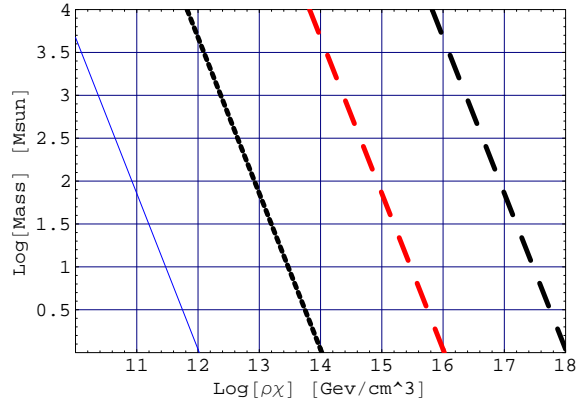


Figure 2: lines on plot correspond to maximum stellar mass due to the Eddington limit as a function of  $\rho_\chi t$  for a fixed cross section. The cross section decreases to the right starting with the cross sections going like  $10^{-37} (cm^2)$ ,  $10^{-39} (cm^2)$ ,  $10^{-41}$ , and the farthest left line corresponds to a cross section of  $10^{-43} (cm^2)$ .

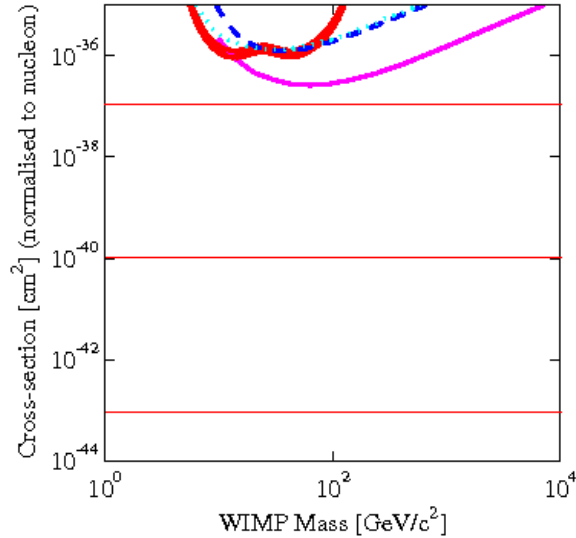


Figure 3: The curve lines correspond to limits set by direct detection limits. Red lines correspond to limits set by not allowing the dark matter luminosity exceeding the Eddington luminosity for a given stellar mass and DM density. If we fix the Max stellar mass to one solar mass, the top line corresponds to a DM density of  $10^{12}(\text{GeV}/\text{cm}^3)$  which is our fiducial cross section of  $10^{-37}(\text{cm}^2)$ , the middle line to a DM density of  $10^{15}(\text{GeV}/\text{cm}^3)$  with a cross section of  $10^{-40}(\text{cm}^2)$  and the bottom line a DM density of  $10^{18}(\text{GeV}/\text{cm}^3)$  with a cross section of  $10^{-43}(\text{cm}^2)$ .



Figure 4: Adiabatically contracted DM profiles for (a) an initial NFW profile and (b) an initial Burkert profile, for  $M_{\text{vir}} = 10^6 M_{\odot}$ ,  $c_{\text{vir}} = 10$ , and  $z = 19$ . The solid (blue) lines show the initial profile. Dot-dashed (black) lines correspond to a baryonic core density  $n \sim 10^7 \text{cm}^{-3}$ , long-dashed (red) lines to  $10^{10} \text{cm}^{-3}$ , dashed (magenta) lines to  $10^{13} \text{cm}^{-3}$ , and dotted (green) lines to  $10^{16} \text{cm}^{-3}$ .